CME LIVE OPEN ACCESS

Journal of
Earth & Environmental Waste Management

Research Article

Mapping Water Pollution Risks and Estimation of Exposed Population in the Case of Upper Awash Sub-Basin, Ethiopia

Tesfa Aklilu[1*], Geremew Sahilu[2], Argaw Ambelu[3], Abdilbasit Hamid[4] and Balew Ybel[5]

[1*]*Ethiopian Institute of Water Resources, Addis Ababa University, Ethiopia.*

[2]*Associate Professor of Civil and Environmental Engineering, School of Civil and Environmental 2Engineering, Addis Ababa Institute of Technology, Addis Ababa University, Ethiopia.*

[3]*Professor of Environmental Health, Ethiopian Institute of Water Resources, Addis Ababa University.*

[4]*Regional Advisor at the federal democratic Republic of Ethiopia Minister of Water and Energy.*

[5]*African Center of Excellence for Water Management, Addis Ababa University.*

Corresponding Author: Tesfa Aklilu, Ethiopian Institute of Water Resources, Addis Ababa University, Ethiopia.

Received: 2024 Mar 27 **Accepted:** 2024 Apr 15 **Published:** 2024 Apr 22

Abstract

Groundwater and surface water pollution risk assessment involves evaluating the potential effects of pollutants on water quality, human health, and the environment. This study focuses on water pollution risks from the intrinsic vulnerability and from population growth, urbanization, industrialization, poor soil and water conservation, climate change impacts, and inadequate governance of Upper Awash Sub-river Basin in Ethiopia. It used Groundwater Pollution Risk Index (GWPRI), Surface Water Pollution Risk Index (SWPRI), integrated Water Source Pollution Risk (WSPR) mapping, water pollution index as well as estimation of exposed population for the identified risks through ArcGIS environment. Linear regression analyzes concentrations of nitrate from 851 boreholes and product map raster values were applied for model validation, achieving a 67.8% explanation (R2=0.678). In addition, Nemerow pollution index was also applied based on samples from ten monitoring sites. As the result, findings reveal 32.96% with low groundwater pollution risk, 53.56% at a moderate risk level, and 13.5% facing high groundwater risk. For surface water, 72.64% has low pollution risk, while 27.36% experiences more than moderate risks, including 4.82% high and 3.7% very high pollution risks. The combined risks shown that 68.1% low, 27.5% moderate, and 4.4% high risks for water source pollution in the sub-basin. The study estimates that 82.52% of the population resides in low WSPR areas, with over 17.47% in moderately risked areas. Furthermore, 5.64%, 3.88%, and 2.30% of the population are exposed to high GWPR, SWPR, and WSPR, respectively. The computed Water Pollution Index values for the dry season exceeded one for all ten water quality monitoring sites, indicating pollution of surface water. In conclusion, WSPR modeling is crucial for identifying vulnerabilities and pollution risks in both new and existing water supply systems. Integrating various approaches and models, coupled with predicting exposed populations for health risks associated with water quality, highlights the importance of considering public and ecosystem health issues in the comprehensive approach of source control, treatment technologies, and regulatory measures.

Keywords: Upper Awash Sub-Basin, Groundwater Pollution Risk Index, Surface Water Pollution Risk Index, Water Source Pollution Risk, Exposed Population, Nitrate Concentration, Nemerow Pollution Index.

1. Introduction

Water quality is a global challenge that affects many aspects of human well-being and environmental sustainability. Developing countries, especially in Sub-Saharan Africa, accessing safe water supply is more difficult due water pollution. This is caused by various factors, such as indiscriminate untreated wastewater disposal, industrialization, urbanization, and agricultural activities. The Upper Awash River Basin is an example of sub-basin that suffers from water quality issues. To address these issues, Integrated Watershed Management (IWSM) is the best strategy, which is considering ecological, social, and economic development, as well as helps mitigate public health problems and promotes overall well-being [1, 2].

It relies on the management of watershed characteristics,

including both biophysical and socio-economic features. Therefore, many water quality parameters can be investigated by considering watershed characteristics, such as climate, spatial and seasonal changes, vegetation, geology, topography, and socio-economic factors [3]. Within the basin system, both flooding, a hydrologic event, and drought characterized by a low flow of water have impacts on the biological, physical, and chemical components of water quality [4]. Change in land use and land cover, including soil erosion, deforestation, changes in cropland and pastures, and urban land use; contribute to deterioration of water quality. Furthermore, improper irrigation management and seepage from reservoirs further affecting the water quality within the system. Moreover, human activities, marked by population growth, urbanization, and increasing construction activities, as well as discharges from industrial zones and mining activities, contribute significantly to the degradation of both surface and ground water.

On the other hand, the characteristics of the watershed, including topography, hydrogeology, soil types, and the impervious surface area, play a crucial role as determinant factors in the natural defense system's protective capacity for ensuring water quality acceptable standards. Topographical characteristics and aquifer media, enabling the transport of contaminants within the groundwater basin, significantly influence the variations in water quality [5]. Hydro-chemical variations in water quality are also regulated by geological, geochemical, and geomorphological factors. In general, the qualities of surface water and groundwater are impacted by geological, physical-chemical, biological, and anthropogenic factors of the watershed [6].

Those characteristics and Water Source Pollution Risk (WSPR) are determined by combining the vulnerability map with land use for the Groundwater Pollution Risk (GWPR) groundwater and surface WPR is modeled through an overlay analysis of watershed characteristics [7]. The DRASTIC model considers parameters such as Depth to water, Recharge, Aquifer media, Soil Media, Topography, Impact of the vadose zone, and Conductivity (hydraulic) of the aquifer [8]. In contrast, GWPR analysis incorporates an additional parameter, the land use index.

On the other hand, the analysis of surface water pollution risks involves assessing topography, soil type, land use and land cover, and watercourse zones to establish surface water pollution risk maps [9]. Furthermore, the level of WSPR is determined by matrix addition, combining both surface and groundwater pollution risk maps to estimate the proportion of the exposed population in each risk class. In other hand, risk models first pinpoint areas of varying groundwater and SWPR with low, moderate, and high areas. Overlaying these areas with population dataand calculating the populations within each risk area is applied in this study to reveal the total exposed population at risks.

Mapping water pollution risks by identifying the vulnerable areas and potential hazards as well as estimation of exposed population. WSPR assessment are important to develop strategies to prevent, reduce, or remediate contamination. This can indicate the overall estimate of the population potentially affected by groundwater and surface water pollution risks. This is crucial for informing decision-makers, policymakers and the public about the potential risks and helping guide appropriate interventions or protective measures. Regular updates and refinement of models based on new data or improved methodologies can enhance the precision of exposed population estimates over time.

Indeed, addressing the deterioration of water quality problem is more effectively accomplished through water resource protection than treatment at the point of us. The Water Safety Plan (WSP) approach by the World Health Organization (WHO) is a source-oriented strategy that involves a system assessment to characterize water quality and quantify associated risks [10]. This evidence-based risk management within IWSM aims to tackle both point and non-point sources of water pollution.

In the Upper Awash Sub-River Basin, the identified characteristics mentioned above serve as contributing factors to the degradation of water quality parameters. The sub-basin is particularly susceptible to water pollution due to these factors, justifying the statement that, overall, the Awash River basin is not only the most important but also the most polluted river basin in Ethiopia [11]. It is even worsen around impacted areas due to industrial areas, settlements and flower farming [12]. The sub-basin accommodates millions of people, featuring numerous industrial zones, varied settlement patterns, emerging towns, high population growth, rapid urbanization, flourishing farms, loss of vegetation, soil erosion, and other significant factors [11, 13].

In addition to these aggravating factors, the major challenges in the Awash Sub-River Basin include a lack of coordination, insufficient evidence, limited attention to source protection and monitoring, failure to integrate water quality issues into water resource management, absence of enforcement mechanisms, and a disconnected institutional setup at the grassroots level [14, 15]. Therefore, even though estimation of exposed population through overlay analysis is limited practice in the study area, this study provide essential evidences for the reduction of risks and the protection of water sources by mapping pollution risks in both surface and groundwater.

The focus includes predicting the proportion of the population exposed to these risks through pollution risk mapping. The findings are valuable contributions to site-specific environmental impact assessments for new developments, aiding in the prioritization of pollution control measures based on identified risk levels, facilitating the establishment of legal regulations related to water quality, and integrating public health considerations into IWSM practices. Additionally, these study findings can serve for appropriate resource allocation and contribute to the delineation of water source protection zones; ensuring effective measures are implemented to safeguard water quality in specific areas.

2. Methods

2.1. Study Area

Awash River basin is one of the Ethiopia's twelve basins, which is extremely significant basin in the country. The Upper Awash Sub-basin is the upper part of the basin, which stands out as aninterestingportion within this network, capturing the complex benefits and challenges faced by the basin. The Upper Awash Sub-basin is located between approximately 8°12'59.39"N to 9°18'00.64"N latitude and 37°06'41.73"E to 39°16'53.09"E longitude. Its topography transitions from 1,500 meters in the east to 3,000 meters in the west, surrounding diverse ecosystems along its 200-kilometer stretch from Ginchi 75km west of Addis Ababa, and ended at Koka Dam. Tributaries like Akaki, Holeta, Berga, and Legedadi nourish the Upper Awash River. A unique climatic pattern dominated in the basin, characterized by vital rainfall from June to September, followed by a drier spell from October to February, and sporadic rainfall occurring between March and May. May is the hottest month, while November and December are cooler months.

Over 65% of the Awash River basin's population, exceeding 9.7 million individuals, reside in the upper awash sub-basin. The sub-basin has population densities ranging from 110 to 270 persons per km2. Addis Ababa, the capital city of the country, finds its home within its boundaries, alongside numerous urban centers blooming diverse industries, agricultural endeavors, and socio-economic activities. Notably, 65% of the nation's industries are located in this sub-basin, and the main basin contains 48-70% of Ethiopia's large-scale irrigated agriculture [16].From which 22.4% of the entire Awash Basin's large-scale irrigated land is existing in the sub-basin [17]. The Upper Awash Sub-basin is selected as a prime study location for various reasons. Its central position, including the capital city, underlines its fundamental role in Ethiopia's socio-economic progress. However, rapid development and urbanization in the area bring unique challenges in managing water sources and preserving the environment. Moreover, the sub-basin faces the hazard of pollution, calling for detailed investigations to safeguard its ecosystems and communities (Figure 1).

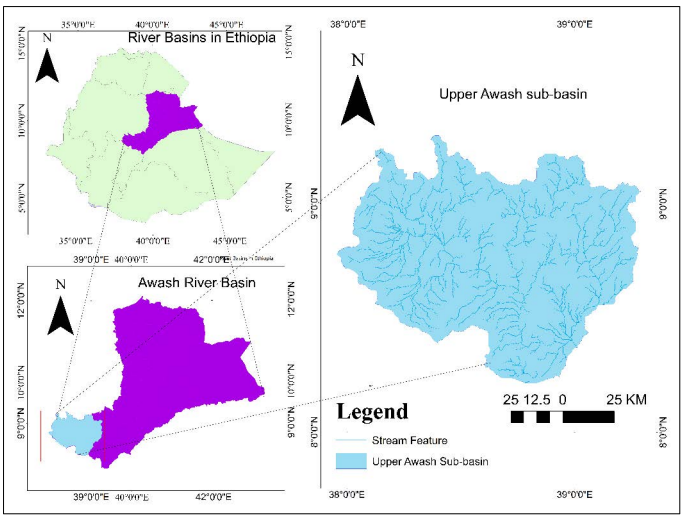

Figure 1: Map of study area, Upper Awash Sub-river Basin.

2.2. Data sources and Model parameters

To map WSPR, various parameters were utilized from different sources. Access to government sources involved acquiring data through official letters, while data from websites, such as satellite images, were obtained through the registration and login process. Depth to the water table (D), effective recharge (R), aquifer media (A), soil type (S), topography (T), impact of vadose zone (I), hydraulic conductivity (C), and Land Use Land Cover (LULC) were obtained from the Ministry of Water and Energy (MOWE). Data on population and settlement maps are sourced from the Water and Land Resource Centre (WLRC) of Addis Ababa University, while information for effective recharge (R) was gathered from the National Metrology Authority (Rainfall data) and MOD16A3GF v006 (MODIS/Terra Net Evapotranspiration Gap-Filled Yearly L4 Global 500 m SIN Grid) [18-20]. Additionally, the Awash River basin Office provides data on land use land cover (LULC). This comprehensive dataset from various sources enables a thorough analysis of parameters in the study area to map WSPR and estimate proportion of exposed population.

2.3. Procedure and Spatial Analysis

In this study, a Geographic Information System (GIS) based analysis was employed, utilizing ArcGIS Version 10.7 to map pollution risk. The process involved overlay analysis of various parameters and the estimation of the proportion of the population exposed to these risks. Figure 2 provides a visual representation of the outlined procedure. For a more in-depth understanding of the methodology and analysis, detailed information is provided in the subsequent sections as follow.

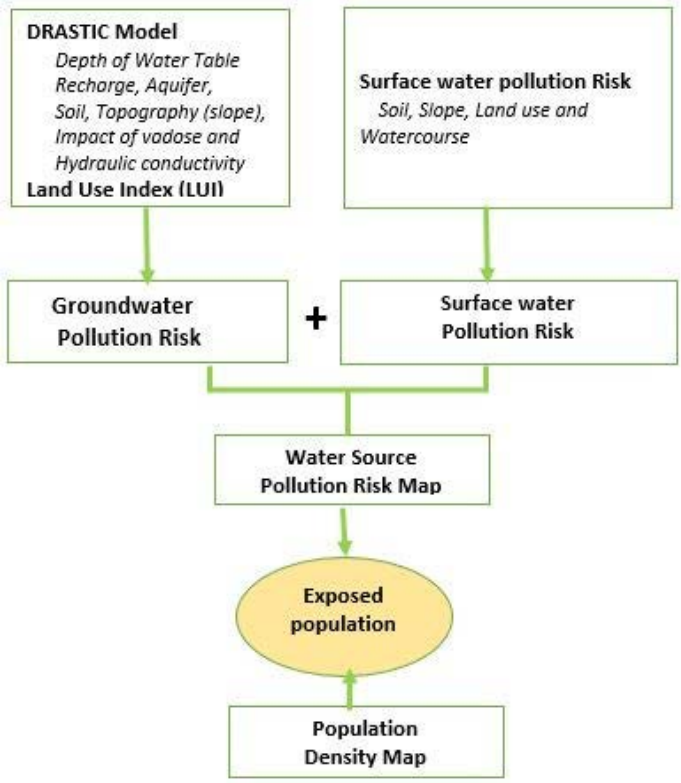

Figure 2: Procedures of ArcGIS Operation for different analysis.

Ciatation:Aklilu, T., Sahilu, G., Ambelu, A., Hamid, A., Ybel, B. (2024). Mapping Water Pollution Risks and Estimation of Exposed Population in the Case of Upper Awash Sub-Basin, Ethiopia. Journal of Earth & Environmental Waste Management. 2(2), 1-16.

2.4. Mapping Groundwater pollution risk

To assess the risk of groundwater pollution, an overlay analysis was conducted using the DRASTIC model index and the Land Use index. The detailed description including:

Depth to water table (D): the interpolation technique was employed to create a raster map of the water table using static water depth of 851 boreholes. This method, widely used for vulnerability assessments of groundwater. The weights for the parameter and the rate values for each class as outlined in Table 2 was determined in accordance with the guidelines of the DRASTIC model [21, 22].

Effective Recharge (R): The calculation of effective recharge involves utilizing input data such as precipitation, evapotranspiration, and land use land cover. To generate the annual precipitation map, 30 years of rainfall data from 13 gauging stations were collected and processed using the These polygon method within the Arc Map toolbox. Annual evapotranspiration and land use land cover raster data were analyzed by using map Algebra within the Arc Map Spatial Analyst extension tool. It was applied to process these raster maps based on equation (1). The recharge ratios, Built areas exhibit a lower recharge ratio of 0.20, suggesting limited permeability and higher surface runoff. Forested areas, on the other hand, demonstrate a higher recharge ratio of 0.73, indicating greater water infiltration and groundwater recharge. Similarly, open fields and lawns display acceptable recharge ratio of 0.75. Agricultural fields, with variations based on soil type, show recharge ratios of 0.60 for clayey soils and 0.70 for sandy soils. These ratios provide valuable insights into the potential impact of land use characteristics on groundwater recharge within the study area. The resulting recharge output raster underwent adjustments in rates and weight to make it suitable for overlay analysis [23].

$$R = (\text{Annual PPT} - \text{Annual ET}) X \text{ Recharge Ratio} \quad (1)$$

Where:
R- Effective Recharge;
Annual PPT- Annual precipitation;
Annual ET- Annual Evapotranspiration.

Aquifer Media (A): The geological shape file was transformed into a geological raster map using the ArcGIS environment to facilitate overlay analysis. Rates were assigned for each class, and the weight for this parameter was determined based on certain criteria (Table 1)

Impact of Vadose Zone (I): as described in the Aquifer media, geological map attribute applied for the estimation of impact of vadose zone. Table 1used for rating classes and weight for impact of vadose zone.

Soil type (S): The soil type map prepared based soil texture map. The rating value of soil type can be given ranging from 10 to 1 for the seven categories of soil type and weight of 2 for soil type parameter (Table 1)

Topography (T): The slope map prepared from digital elevation map. Slope values can be grouped into seven classes and rating value ranges from1 to 10 (Table 1).

Hydraulic Conductivity (C): its raster map prepared using the geological nature of the aquifer of the sub basin, as it is possible to use information of aquifer media in the absence of unavailability of hydraulic conductivity data. Estimated hydraulic conductivity helped to provide rating for each geological material [24].

Land use land cover (LULC): The Land us Index (LUI) calculated based on equation (2) and the weight for land use and land cover taken as 5 and the rating value is described in Table 1

$$LUI = Lr \times Lw \quad (2)$$

Where;
LUI: Land use index;
Lr: Land use rating;
Lw : Land use weight

DRASTIC modeling: the simulation of DRASTIC modeling was conducted using the Spatial Analyst extension within ESRI's ArcGIS 10.7 software. This tool, specifically the Spatial Analyst in ArcGIS, enables the processing of various digital map layers to delineate vulnerable zones by calculating the vulnerability index and analyzing the spatial variability of groundwater vulnerability [21]. Each DRASTIC parameter and other digital geospatial datasets for the model were created using collected shape file formats within the ArcGIS environment. Vector formats were converted into raster, and weights and rates were assigned to the parameters. Employing raster calculator and Lookup syntax in the ArcGIS 10.7 environment, overlay analysis of the parameters was performed to generate DRASTIC and Land Use Index (LUI) based on equation (2) and (3). The DRASTIC map product has been categorized into four classes to interpret vulnerability levels: low vulnerability with values less than 109, moderate vulnerability ranging from 109 to 138, highly vulnerable between 138 and 166, and very highly vulnerable for values above 166, as derived from the processed raster map.

Table 1: DRASTIC and Land use Index rating and weight values.

Rating	Depth of water table(m) W= 5	Net Recharge (mm/y) W= 4	Aquifer Media, W=3	Soil Media W=2	Topography (%), W=1	Impact of Vadose Zone W=5	Hydraulic Conductivity (GPD/ft2) W= 3	LULC categories (weight =5)
10	0.0 -1.5		Karst Limestone	Thin or absent, gravel	0-2	Karst Limestone	>2000	Croplands
09	1.5 - 4.5	>250	Basalt	Sandstone & volcanic	2-6	Basalt		Built-up areas
08		180-250	Sand & Gravel	Peat		Sand and Gravel	1000-2000	Urban areas
07	4.5 - 9		Massive Sandstone and limestone	Shrinking/ aggregate clay/alluvium		Gravel, sand		Non-irrigated field crops
06		100-180	Bedded sandstone and lime stone	Sandy loam, schist, sand, karst volcanic		Limestone, Sandstone, Sand and Gravel with Silt & clay	700-1000	
05	9 -15		Glacial	loam	6-12			
04			Weathered Metamorphic/igneous	Silt loam		Metamorphic/ igneous	300-700	Grassland/ scrublands
03	15 - 23	50-100	Metamorphic/Igneous	Clay loam	12-18	Shale		Water bodies
02	23 - 31		Massive Shale				100-300	
01	>31	0.0-50		Non-shrink & Non-aggregated clay	>18	Silt/Clay	1-100	Bare areas/ uncultivated Forest/ tree/

$$DIV = Dr * Dw + Rr * Rw + Ar * Aw + Sr * Sw + Tr * Tw + Ir * Iw + Cr * Cw \quad (3)$$

Where:
DIV= DRASTIC Index Value
r = rating for the parameter
w = given weight for the parameter
D: Depth to Groundwater
R: Net Recharge
A: Aquifer Media
S: Soil Media
T: Topography (slope)
I: Vadose Zone
C: Hydraulic Conductivity of the Aquifer

Groundwater Pollution Risk Index: The final GWPR map was generated using a map algebra function, combining the DRASTIC Value Index and the Land Use Index (LUI) through Equation (4). The GWPR Index Values from the resulting raster map were further classified into four risk classes: Low, Moderate, High, and Very High. The GWPR classes are defined by total index values, with a categorization into four levels. A total index value below 165 corresponds to the low-risk class, while values ranging from 166 to 207 fall into the moderate-risk category. The high-risk class encompasses total index values between 208 and 249, and any value exceeding 270 is classified as very high risk. This classification system serves as a useful tool for assessing and categorizing the severity of groundwater pollution risks, providing a clear and concise framework for understanding and managing groundwater quality within the study area.

$$WPRI = DVI + LUI \quad (4)$$

Where:
GWPR: Groundwater Pollution Risk Index;
DVI: DRASTIC Value Index and
LUI: Land Use Index

2.5. Surface Water pollution risk

The prediction of SWPR involves the combination of four parameters based on equation (5). These parameters, namely Soil type, Slope, Land Use Land Cover, and Watercourse raster maps, were assigned weights based on findings from similar studies [24, 25].The nature of each parameter was analyzed using ArcGIS toolbox. Soil type, Land Use Land Cover, and Slope underwent processing to obtain rated raster maps for subsequent analysis. Furthermore, the watercourse parameter was derived using the multiple ring buffer tool, following a series of steps utilizing the hydrology tool from Digital Elevation Model (DEM) data. The streams were then classified into four buffering rings or zones, as outlined in Table 2, specifying the parameters and their rates for surface water pollution risk estimation [26].

Table 2: Class and rate of each factors of SWPR.

S/N	Soil type		Slope (%)		Land use		Watercourse (W) [in m]	
	Class	Rate	Class	Rate	Class	Rate	Class	Rate
1	Clays	5	>14	30	Agriculture (Cropland)	20	Zone 1 (0–50)	10
2	Silts/fine sand	4	11–14	21	Barren land	8	Zone 2 (50–200)	6
3	Sands	3	8–10	13	Settlements/ Urban areas	6	Zone 3 (200-1000)	3
4	Organic matter	3	5–7	8	Shrub/ bush/ Woodland	4	Zone 4 (>1000)	0
5	Gravels/ hard rock	2	3–4	4	Grassland	2		
			1–2	2	Forests	1		
			0	1	Water body	1		

The equation for the production of the final SWPR map is described in as:

$$WPS = K \times S \times W \times U \quad (5)$$

Where:
SWPR: Surface Water Pollution Risk
K: Soil type (Texture)
S: Slope in percent
W: Watercourse (Buffer)
U: Land Use

The final overlay analysis classified in to four risk classes using mean values of the product and standard deviation [27]. The low-risk class corresponds to total index values below the mean, while the moderate-risk class includes values from the mean to one standard deviation above the mean (Mean plus 1SD). The high-risk class encompasses total index values falling between the mean and two standard deviations above the mean (Mean plus 2SD). Lastly, the very high-risk class comprises values greater than the mean plus three standard deviations (Mean plus 3SD). This classification system based on mean and standard deviation provides a concise and quantitative framework for assessing different levels of risk, offering a standardized approach to understanding GWPR within the study area.

2.6. Water pollution Risk modeling

Within the ArcGIS framework, the assessment of contamination risks for both ground water and surface water was conducted to determine water-source pollution risks (figure 2). The matrix addition resulted in the creation of eight classes on the raster map, subsequently categorized into three risk levels: low with values 2 and 3, moderate with values 4 and 5, and high risk with values 6, 7, and 8.

2.7. Exposed Population Analysis

In the ArcGIS environment, the population map was generated using the raster layer of the 2016 population density model. The population density raster specific to the Upper Awash sub-basin was extracted through masking. To estimate the exposed population in the zone of GWPR, SWPR, and WSPR maps, the Zonal Statistics (Spatial Analyst) tool of ArcGIS environment was employed. This tool calculated statistics and summarized the values of a raster within the zone of anther raster and report as table. Accordingly, it used the values of the population density raster map within the zones defined by the three aforementioned raster (GWPR, SWPR, and WSPR) maps (Figure 2). Further calculations, involving the proportion or absolute number of people exposed to water pollution risks or residing in different statuses of water pollution risks, were carried out using Microsoft Excel 2016.

2.7. Model Validation

The validation process utilized Nitrate concentrations and raster values, with Nitrate chosen due to its contaminant nature in groundwater [21]. Extracting raster values from the DRASTIC model-generated map and linking them with point data from 851 boreholes were performed using the Extract Raster Values to Point tool in ArcGIS. This generated

new data for simple regression analysis, validating the model against ground truth. SPSS version 25 facilitated statistical analysis, comparing raster values with observed nitrate concentrations. Nitrate concentration served as the dependent variable, while raster values were considered independent [Equation (1)].The assumptions of normality, linearity, homoscedasticity and independence for linear regression analysis were satisfied. The model's goodness of fit was assessed through the coefficient of determination (R-Square). It signifies the proportion of total variation in the dependent variable explained by variations in the independent variable. The remaining percentage reflects unexplained variations in nitrate concentration attributed to factors not considered in the DRASTIC Value Index.

$$Y_i = \beta_o + \beta_1 X_i + \varepsilon_i \qquad (6)$$

Where Y_i is dependent variable (Nitrate concentration, mg/l), β_o is Population Intercept, β_1 is Population Slope Coefficient, X_i is independent variable (raster values) and ε_i is random error term.

2.8. Water pollution index

In this research, the methodology incorporates the utilization of a water pollution index to comprehensively evaluate the overall health of a water body within the sub-basin. The Nemerow pollution index is specifically employed to assess the degree of surface water pollution, serving both as a quantitative measure and as a validation tool for the broader Water Source Pollution Risk (WSPR) assessment. Surface water data, systematically collected in 2021 from ten river water-sampling stations located within the sub-basin, were obtained through the Ministry of Water and Energy (MOWE) for monitoring surface water quality. The collected dataset was prepared for analysis using MS Excel 2016 software based on Equation (7). A comprehensive data management process resulted, including checks for missing data, treatments for outliers, and general data cleaning procedures. Subsequently, the average values for both dry and wet seasons were computed for further analysis and interpretations.

$$WPI = \sqrt{\frac{[\left(\frac{1}{N}\right)\sum\left(\frac{Ci}{Si}\right)]^2 + [\mathrm{Max}\left(\frac{Ci}{Si}\right)]^2}{2}} \qquad (7)$$

Where
WPI: Water Pollution Index.
N: number of water quality parameters being considered.
Ci: concentration of the I Th parameter in the water sample.
Si: standard or permissible limit for the I Th parameter.
Max: maximum concentration

The index has six categories, each with a different range of numbers: no pollution (up to 0.5), clean (0.5 to 0.7), warm (0.7 to 1.0), polluted (1.0 to 2.0), medium pollution (2.0 to 3.0), and severe pollution (above 3.0). The index can be used to evaluate the ecological condition and health risk of a water body, and to suggest ways to improve water quality.

3. Results and discussions

This study aims to map water pollution risks in the Upper Awash River Sub-Basin and predict the number of exposed populations using ArcGIS. The research provides evidence for effective risk reduction and source protection strategies in water quality, land, and urban management. Various factors influencing water quality at the watershed scale are analyzed and described in the subsequent sections.

3.1. Validation of DRASTIC Model

Model validation is a crucial step to evaluate the model results. As the result, in the model validation using linear regression, assumptions of normality, linearity, homoscedasticity and independence were checked using visual inspection of graphs and tests, for instance, the Durbin-Watson test (1.7) is in the acceptable range of 1.5 to 2.5 that indicate independence between the targeted variable (Table 3).

Table 3: Results of linear regression analysis for Mode validation.

Descriptive Statistics	Variables	N	Mean	Std. D		
	Nitrate (mg/l)	851	8.30	11.19		
	Index value	851	136.86	24.98		
Model Summary	**R^2**	**F Change**	**df1**	**df2**	**Sig.**	**Durbin-Watson**
	0.678	1788.845	1	849	0.000	1.711
ANOVA		Sum of Squares	df	Mean Square	F	Sig.
	Regression	72156.86	1	72156.86	1788.85	0.000
	Residual	34246.22	849	40.34		
	Total	106403.08	850			
Coefficients	**Unstandardized**	**t**	**Sig.**	**95.0% CI for B**		
	B			**Lower Bound**	**Upper Bound**	
	- 42.185	-34.771	0.000	-44.566	-39.80	
	0.369	42.295	0.000	0.352	0.386	

The Model Summary reveals that 67.8% of the variance in the dependent variable, nitrate concentration, is explained by the independent variable, raster values of the DRASTIC index. The significant P-value in the ANOVA table (P<0.001) ensures that the regression model predicts the dependent variable better than chance. The Coefficients table provides values for the equation (1) to predict nitrate concentration from raster values. Within the 95% Confidence Interval for B, the intercept is -42.19, and the slope is 0.37, indicating a parameter value for the slope of the regression line between 0.352 and 0.39. The validation process using nitrate concentration in the DRASTIC model confirms its effectiveness in assessing water pollution risk. Nitrate concentrations exceeding 2mg/l, attributed to human activities, revealing a strong association with pollution risk indices explained by 67.8% [28].The validation produced a predictable model, for every one unit of increase in groundwater vulnerability index; the nitrate concentration could be increased by 0.37 units. Consequently, the DRASTIC model's input parameters are validated and accepted [29].In other hand, correlations were observed between cropland percentage, temperature, and precipitation with negative impacts on nitrate concentration [30].Positive correlations were found between nitrate concentration in the Vadose zone and increased groundwater depth due to Denitrification processes [31, 32]. Nitrate sources in groundwater, whether natural or anthropogenic, contribute to varying concentrations [33].The study aligns with the report from the Awash River Basin, indicating elevated nitrate concentrations in the upper Awash River sub-basin compared to other catchments, verifying the study's mean concentration of 8.30mg/l [34].

3.2. Water pollution Index

In the calculation of the Water Pollution Index (WPI), fifteen water quality parameters were considered. The analysis revealed notable variations in the mean values of these parameters between wet and dry seasons. Specifically, during the dry season, nine parameters (TDS, pH, TH, Ca, Mg, HCO3, F, NO3 and Cl) exhibited higher mean values, while six parameters (Na, K, Fe, Mn, NO2, and SO4) demonstrated elevated mean values during the wet season (Supplementary #1).

The computed WPI values for the dry season exceeded 1 for all ten monitoring sites, indicating pollution of surface water. Among these, two sites were categorized as polluted (1.0 to 2.0), three exhibited medium pollution levels (2.0 to 3.0), and five were characterized by severe pollution (above 3.0) (Table 4). These findings highlights the urgent need for remedial measures to enhance water quality, emphasizing the importance of addressing ecological conditions and mitigating health risks associated with the river water in the targeted sub-basin.

Table 4: Water pollution Index of ten river water quality-monitoring stations.

S/ N	Water Quality Monitoring Station	Seasons of the year	
		Dry season	Wet Season
1	Koka	1.78	1.26
2	Zeway	2.50	1.47
3	Modjo	3.86	1.24
4	Ginchi	1.39	2.21
5	Great Akakie	2.43	1.39
6	After Abasamuel	4.98	0.78
7	Legedadi	1.70	0.85
8	Melkakunter	3.23	1.31
9	Little Akakie	4.96	0.94
10	Ombolie	2.17	3.68

The research, employing the WPI in various locations, provides valuable insights into diverse water quality conditions and concerns across ecosystems. In Greek rivers and lakes, study reveals moderate to high pollution levels, emphasizing an urgent need for environmental intervention [35]. Similarly, the WPI demonstrates a significant correlation between pollutant concentration and water quality management, offering crucial insights for prioritizing effective management measures [36]. In Basrah Marshes, Iraq, undesirable physico-chemical parameters result in elevated Water Pollution Index values, categorizing the water as not clean and highlighting critical environmental challenges [37]. Investigations in the Yangtze River and Yellow River Basins in China underscore the complex impact of increased pollution, with variations observed between basins and seasonal influences on agricultural pollution [38]. The correlation between the water pollution index and the incidence of diarrhea in children under five years old in the coastal area of Semarang City, Indonesia, underscores the critical health implications of water quality, emphasizing the necessity for comprehensive water quality management [39].

In contrast, the Alaknanda River in Uttarakhand, India, consistently maintains good water quality conditions throughout the year, as evidenced by the WPI [36]. Similarly, the investigation of Heilongtan reservoir in China reveals stable water quality over three years, with minimal temporal and spatial changes, implying effective water quality man-

agement practices [40]. In Dramaga Campus in Indonesia, utilizing pollution index, suggests a favorable water quality status [41]. Despite exhibiting low pollution levels, the Ganges River in Bangladesh underlines the importance of implementing proper management and monitoring strategies for sustainable use [42]. Lastly, the evaluation of Lugu Lake in China, employing Nemerow pollution index and single-factor pollution index methods, consistently indicates good water quality conditions over three years, pointing to effective environmental management [43].

In general, this study and others conducted globally demonstrate the utility of the WPI in assessing water pollution status. The WPI serves as a valuable tool for enhancing water quality and mitigating the adverse effects of water pollution. For instance, evaluations of groundwater quality in China, Indonesia, and Egypt, incorporating pollution indices such as Nemerow and DRASTIC models, unveil the complex influence of pollutants and aquifer vulnerability. These assessments offer crucial insights for sustainable groundwater management [44]. The utilization of the WPI for groundwater vulnerability mapping in Datong City, China, emphasizes the importance of integrated approaches in evaluating groundwater quality, especially in regions with limited data [45].

3.3. Ground Water Pollution Risk

In the designated sub-basin, an integrated approach combining the DRASTIC model and land use index is employed for predicting groundwater pollution risks. This model, developed from governing equations and a weighting system involving eight parameters through overlay analysis, provides a comprehensive assessment that facilitates the prioritization of groundwater protection measures [46]. It effectively captures the impact of human activities such as agriculture, urban planning, industrial development, and deforestation/afforestation on water quality. The method utilizes standardized land use ratings and weights to generate risk maps, which are theninterpreted based on four classes of risk levels. As a result, approximately 32.96% of the sub-basin falls into the low GWPR category, while 53.56% is classified as having a moderate risk level (Figure 3). Furthermore, more than 13.5% of the sub-basin is identified with a high groundwater risk level table 5. This approach provides valuable insights for targeted intervention and management strategies to mitigate groundwater pollution.

Table 5: Groundwater Pollution risk level, Upper Awash Sub-basin.

S/N	Risk Levels	Area (m^2)	%
1	Low Risk (77-165 value)	3528673200	32.96
2	Moderate (166-207 value)	5734532700	53.56
3	High Risk (207 – 249 values)	1440726300	13.46
4	Very High Risk (249-256 values)	3491100	0.03
	Total	10707423300	100

Groundwater quality is subject to the influence of geological, physico-chemical, biological, and anthropogenic factors. Notable anthropogenic contributors encompass municipal waste dumpsites, sewage effluent, and agricultural fertilizers. Hydro-geochemical characterizations, water-rock interactions, and the mixture of waters through geochemical processes are hydrogeological factors contributing to groundwater pollution [47]. The DRASTIC model, rooted in physical characteristics affecting groundwater pollution potential. These physical characteristics include depth to water, net recharge, aquifer media, soil media, topography, impact of the vadose zone, and hydraulic conductivity of the aquifer [8].

The depth of the water table plays a crucial role in the infiltration of pollutants within the aquifer's unsaturated zone, with shallower depths indicating increased vulnerability to contaminants. The recharge process facilitates the transport of surface pollutants into the subsurface. Higher net recharge in the aquifer corresponds to an increased likelihood of contaminating the water table [21]. It is influenced by precipitation, evapotranspiration, and land use characteristics, resulting in variable recharge ratios. A precipitation raster map was generated using interpolated data from 13 meteorological stations over a 30-year period. Evidence indicates a significant proportion of groundwater recharge in the Middle Blue Nile basin, contributing to the storage of aquifer systems in the Upper Awash basin [48]. The aquifer medium serves as a subsurface water storage unit and facilitates the transport of contaminants within it, with the speed of transportation being determined by the aquifer type [49, 50]. In areas where the aquifer system has low retardation and filter percolating fluid capacity, it becomes highly vulnerable to surface contamination [51]. In addition to vulnerability characteristics, the types and loads of contaminants play influential roles in groundwater pollution, ultimately influencing the choice of protective measures [52].In the southern part, the upper and lower regional basaltic aquifers combine to form an unconfined regional aquifer system, while the lower and upper systems are separated by a regional aquiclude, resulting in confined aquifers in the northern and central parts of the sub-basin [53]. On the other hand, the Vadose Zone serves as the connector in the hydrologic cycle between the surface component and groundwater, influenced by factors such as texture, mineral composition, grain size, and fracturing [22, 49, 50]. It acts as the protective zone for groundwater and is the region between the ground surface and the water table aquifer media. The impact of storm water infiltration systems on groundwater is contingent on the thickness of the vadose zone, as distinct biogeochemical

processes occur within it. Parameters such as water transit time and water saturation of the vadose zone are crucial for bacterial transfers associated with infiltration [54].

Hydraulic conductivity quantifies the ease with which a fluid moves through the pore space of an aquifer, determining the potential movement of contaminants in the saturated media through the interconnectivity of voids within the aquifer. A higher hydraulic conductivity rate indicates greater vulnerability of the aquifer to groundwater pollutants [55]. Various physicochemical processes of the soil, such as sorption, ionic exchange, oxidation, or biological activity, affect the transportation of pollutants and serve as the primary defense against contaminants entering groundwater. The soil type parameter is mapped using a digital soil texture map and assessed for its ability to retain pollutants with seven classes [22, 49, 50]. A gentle slope facilitates the movement of pollutants from the ground surface to the groundwater, whereas areas with a steeper slope tend to generate more runoff, reducing the infiltration of contaminants into the groundwater [22, 49, 50]. Additionally, the land use and land cover on the ground surface are significant factors affected by land degradation, which, in turn, has repercussions on water quality [56]. Activities such as soil erosion, sediment deposition in water bodies, deforestation, and changes in cropland and pastures contribute to the deterioration of water quality [57]. Furthermore, inadequate irrigation management and reservoir seepage can result in the contamination of groundwater quality [58].

Deteriorated water quality is evident downstream, primarily influenced by dominant urban land use and point source water pollution [59]. Various anthropogenic factors, including high livestock density, grazing animals, pasture productions, and other land use activities, contribute significantly to water quality issues [60, 61]. Within the sub-basin, there is a noticeable trend of increased cropland utilization and urban expansion, contrasting with the inadequate maintenance of vegetation covers. Land use and cover changes have led to substantial fluctuations in streamflow and sediment yield [62]. The accelerated rates of deforestation, population growth, urbanization, and cropland expansion have adversely impacted both available water resources and the stipulated water quality parameters [63]. These findings emphasize the imperative for future improvements in land use and cover, emphasizing the necessity for the development of effective basin management strategies.

Addressing groundwater pollution proves challenging, necessitating the safeguarding of groundwater sources by implementing risk reduction measures within the watershed management framework. Key solutions involve delineating groundwater vulnerability and mapping protection zones. This approach serves to minimize the probability of hazard release, mitigate the consequences of hazards, reduce residual risks of groundwater contamination, and identify the weakest barriers for effective risk management [64]. Evidence from the sub-basin areas underscores the influence of geogenic processes and anthropogenic activities, such as urban sewage and fertilizer use, on the groundwater chemistry in the study area [65]. It is noteworthy that, aside from land use, the risk of water contamination may be attributed more too poor well construction and casing corrosion. This underscores the need for designing risk management actions that take into account well designs and operational practices. By combining the vulnerability index with the land use characteristics of the area, it becomes possible to rank groundwater pollution risks through the spatial distribution of vulnerability and risk. This ranking serves as a foundation for implementing measures aimed at the protection, restoration, and integrated management of groundwater resources [66]. The prioritization of vulnerability areas within the sub-basin facilitates focused groundwater monitoring and the prevention of groundwater contamination. Additionally, GWPR mapping functions as a valuable decision-making tool, supporting hydrogeological conceptualization and the decision-making process in water resources management.

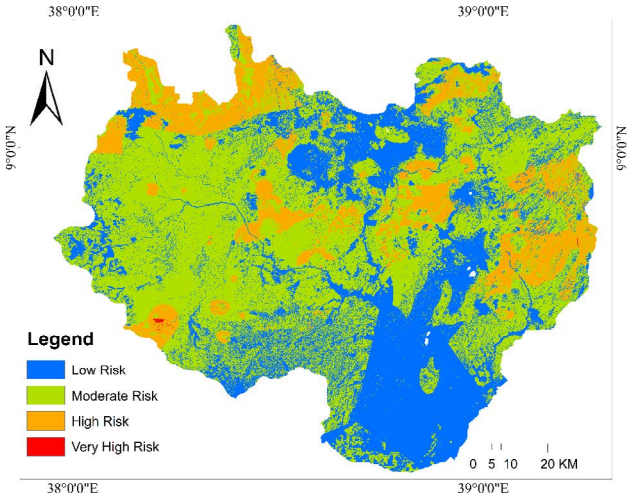

Figure 3: Map of GWPR in Upper Awash Sub-basin.

Research indicates a moderate vulnerability to groundwater pollution from pesticide use due to their rapid dissolution and penetration into groundwater. In Lahore, Pakistan, the model highlighted high vulnerability in land use, development, industrial, and agricultural areas compared to settlements [9].The Haouz aquifer in Morocco displayed the model's ability to differentiate between vertical vulnerability(vadose zone) and contamination susceptibility (saturated zone) [67]. In India, the DRASTIC model demonstrated a strong correlation with nitrate levels, particularly suitable for assessing agricultural nonpoint source pollution. Groundwater pollutants encompass biological, inorganic, and organic categories, originating from various sources such as municipal waste dumps (Lagos, Nigeria), hydrogeochemical characteristics (Janah Plain, Iran),sewage, fertilizers, and water-rock interactions (Nandong karst system, China), evaporation, water-rock interaction, and water mixing (Central Morocco), and industrial, urban effluents, and agricultural activities (Serbia) [47, 67-69]. Overall, these findings underscore the effectiveness of the DRASTIC model in evaluating groundwater vulnerability and pinpointing areas at risk from diverse pollution sources. Recognizing these vulnerabilities is vital for implementing robust water resource management and protection strategies. Therefore, the application of this

model, which assesses groundwater vulnerability to pollution based on hydrogeologic parameters without extensive site-specific pollution data, emerges as a cost-effective method to identify areas necessitating further investigation, such as risk assessment studies.

3.4. Surface Water pollution Risk

SWPR modeling is crucial for safeguarding water bodies. This involves ArcGIS overlay analysis, considering watershed characteristics that influence water quality parameters. Some models rate these characteristics to assess the risk of potential contamination to water supplies. In the Sub-basin, integrated models manage land, sedimentation, and nutrients, assisting in delineating protection zones. Incorporating a geographical information system enhances SWPR modeling, enabling the creation of watershed-scale risk maps for nonpoint source pollution. Notably, this approach can be regularly updated in response to observed parameter changes [70].

Table 6: Surface Water Pollution risk level, Upper Awash Sub-basin.

S/N	Risk Levels	Area (m^2)	Percentage (%)
1	Low Risk (3- 780 value)	7,798,175,100.00	72.64
2	Moderate (780-2170 value)	2,022,706,800.00	18.84
3	High Risk (2170-3560 values)	517,353,300.00	4.82
4	Very High Risk (3560 -30000 values)	396,855,000.00	3.70
	Total	10,735,090.200	100

Following this model approach, the study affirms that merely 72.64% of the sub-basin exhibits a low SWPR level (Figure 4). Contrastingly, 27.36% of the sub-basin comprises areas with more than moderate risk, with approximately 4.82% classified as high pollution risks and 3.7% as very high pollution risks (Table 6).Notably, a study conducted in Ethiopia assessing surface water risk indicated a low to negligible acute human risk associated with surface water consumption [71]. However, in contrast, concentrations of selected nutrients and heavy metals were found to be consistent among the sampling sites along the streams of the sub-basin, attributed to pollution from catchment nutrient sources [72].

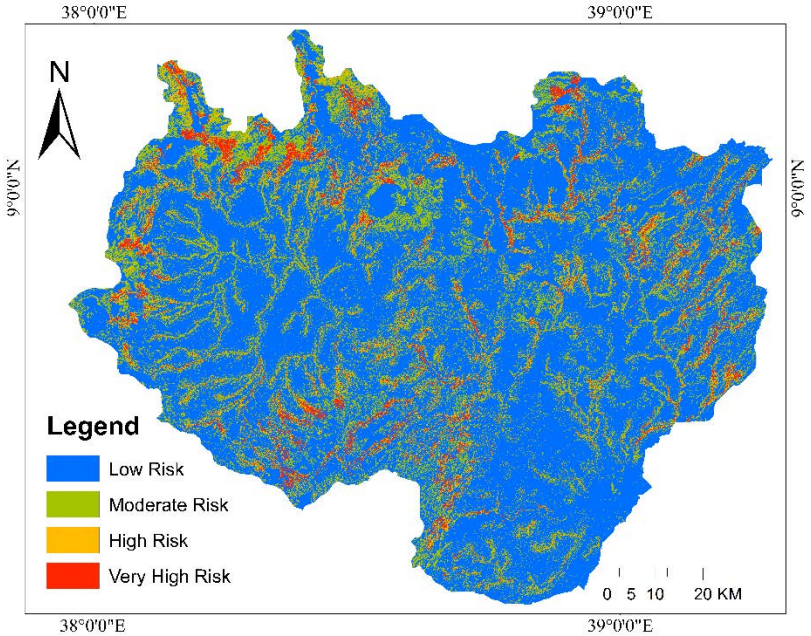

Figure 4: Surface Water pollution risk, Upper Awash Sub-basin

3.5. Water Source Pollution Risks

Water pollution is characterized by the presence of excessive amounts of pollutants in water to the extent that it becomes unsuitable for drinking, bathing, cooking, or other purposes [73]. The evidence highlights four major pollution sources: industries, mining and related activities, mixed sources (geogenic and anthropogenic), and fertilizer application [74]. In this study, separately modeled groundwater and surface-water pollution risk maps were integrated to create unified risk rating maps through a matrix addition operation within the ArcGIS environment. Consequently, the product map delineates seven risk classes (Table 6), which were further reclassified into three classes (Table 7). As per Figure 5, the sub-basin area is classified as 68.1% low risk, 27.5% moderate risk, and 4.4% high risk for water source pollution (Table 8).

Table 7: Water source (ground and surface) Pollution risk level, Upper Awash Sub-basin.

S/N	Risk Levels	Area (m^2)	Percentage (%)	Remark (Matrix addition of values)
1	Risk Level 2	3,092,021,100.00	28.8774	1,1&1,1
2	Risk Level 3	4,199,048,100.00	39.2162	1,2 & 2,1
3	Risk Level 4	2,159,873,100.00	20.1717	2,2; 2,2; 3, 1 & 1, 2
4	Risk Level 5	783,423,900.00	7.3166	2,3;3,2 and 1,4
5	Risk Level 6	367,049,700.00	3.4280	4,2; 2,4; 3,3 & 3,3
6	Risk Level 7	105,939,000.00	0.9894	3,4 & 4,3
7	Risk Level 8	68,400.00	0.0006	4,4 & 4,4
		10,707,423,300.00	100.0000	

In the study area, evidence suggests that the conjunctive use of surface and groundwater could enhance water supply and alleviate stresses on groundwater resources. To implement this approach effectively, understanding SWPR is crucial for addressing water quality issues. This also supports a source protection strategy to prevent contaminants from entering surface waters, aquifers, or groundwater recharge areas. However, in the sub-basin, Integrated Water Resources Management (IWRM) principles and economic development plans were not implemented with due consideration for equity and the environment [75].

Table 8: Reclassified WPR levels, Upper Awash Sub-basin.

S/N	Risk Levels	Area (m^2)	%	Remark (classification of values)
1	Low Risk	7,291,069,200.00	68.1	1,2 & 3
2	Moderate Risk	2,943,297,000.00	27.5	4 & 5
3	High Risk	473,057,100.00	4.4	6,7 & 8
	Total	10,707,423,300.00	100	

Therefore, this study advocates for the application of a multiple barriers approach, which identifies critical sites for contaminants' entry into the drinking water supply system [76]. This involves a risk management system by developing a water safety plan approach, which can help control contamination risks, comprehend the risks associated with the process, and identify Critical Control Points to integrate within water supply operations [77].

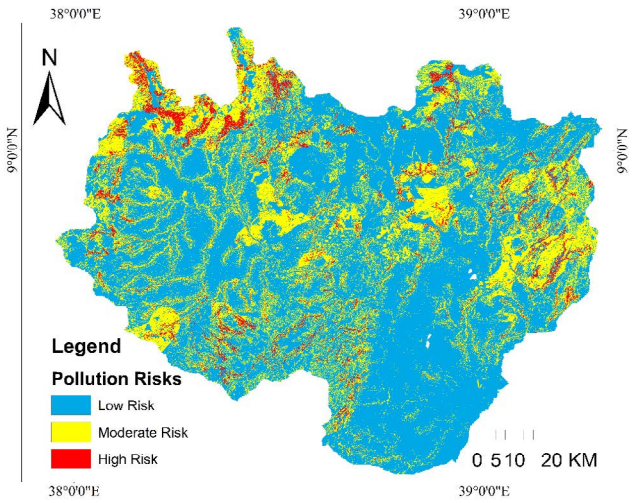

Figure 5: Water source pollution risk, Upper Awash Sub-basin.

3.6. Exposed Population for water pollution risks

The estimation of the population residing in WPR areas was conducted by utilizing population density maps (number of persons per square kilometer, 2016 CSA) and a WPR map. This was achieved through the ArcGIS zonal statistic method within the tool sets. The results reveal that 82.52% of the population (3,663,891 persons) resides in areas characterized by low water pollution risk, while more than17.47% live in moderately risk-prone areas. Notably, a higher proportion of individuals are exposed to more than moderate risk when considering both groundwater and surface water pollution risks (Table 8). An estimation of 5.64%, 3.88% and 2.30% of the population were exposed for high GWPR, SWPR and WSPR respectively. It is essential to recognize that water supplied from defined moderately and high-risk areas may serve as a water source for individuals residing in low-risk areas. Therefore, in addition to predicting water source risks, it is imperative to track drinking water supply sources with respect to the WPR product map for comprehensive water quality management within the watershed system.

In Ethiopia, high rural population density correlates with smaller farm sizes and increased fertilizer use per hectare, potentially leading to water pollution if fertilizer application is not managed wisely [78]. The assessment of heavy metals in the A wash basin's surface water emphasizes the need for measures to reduce pollution risks in accordance with basin standards [79]. Severe surface water quality impairment is observed in the upper A wash basin, where over 90% of

Addis Ababa's industries discharge untreated waste into nearby waterways [80].The heavy metal evaluation index indicates elevated levels of Fe, Mn, and Cr in groundwater, posing a serious threat to the exposed population [81]. Water pollution in Ethiopia is a major concern for public health and water security, stemming from human activities and weak enforcement, with limited understanding of the effectiveness of policies and institutional frameworks in addressing pollution [82].

Table 9: Exposed population and Water Pollution risk levels, Upper Awash Sub-basin.

S/N	Risk Level	GWPR level		SWPR level		WPR (combined)	
		Population	%	Population	%	Population	%
1	Low	2483266	55.93	3,603,915	81.11	3663891	82.52
2	Moderate	1706278	38.43	548,731	12.35	673680	15.17
3	High risk	250248	5.64	172,305	3.88	102018	2.30
4	Very High Risk	245	0.01	118,484	2.67	-	-
		4,440,037	100	4,443,435	100	4,439,589	100

Studies on human health risks due to water pollution highlight the scientific understanding required for the biological, chemical, and physical processes controlling contaminant movement, with consequences varying based on factors such as composition, exposure duration, and pollutant concentration [83].

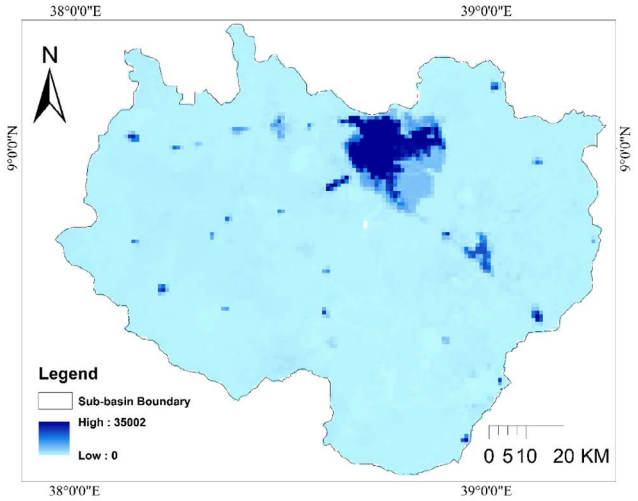

Figure 6: Population Density (Number of person/Km2), Upper Awash Sub-basin.

Research on the impacts of land use and population density on seasonal surface water quality suggests that urban land is a dominant factor influencing pollutants in highly urbanized regions, with the relationship being weak as pollutants primarily come from point sources [84]. By the late twentieth century, population growth was causing increasing constraints on land, water, and other natural resources in many areas [85]. The changing land use and population density are identified as factors degrading water quality in the Lower Mekong Basin, associated with agriculture, urbanization, and population density. Population exposure assessment in water pollution is crucial as it directly affects public health by helping to understand and mitigate the risks associated with contaminated water sources. Identifying areas with high exposure allows for targeted interventions, aiding in the prevention of waterborne diseases and ensuring environmental justice by addressing vulnerabilities in specific communities. Moreover, it facilitates regulatory compliance, guiding policymakers to enforce measures that improve water quality and protect public health. Efficient resource allocation is enabled by prioritizing interventions in areas most at risk, while community awareness and empowerment are fostered through sharing assessment results, enabling informed decision-making. Ultimately, population exposure assessments contribute to the development of sustainable water management strategies, addressing immediate pollution concerns and laying the foundation for long-term water quality improvement and resource preservation for future generations.

4. Conclusion

The assessment of surface water and groundwater pollution risks, along with the computation of the Water Pollution Index (WPI), reveals alarming findings that highlight the severity of water pollution in the studied areas. Moreover, the estimation of the proportion of the exposed population to different pollution risk levels contributes significantly to understanding and addressing these risks, offering essential information for implementing source protection measures. The study findings indicate that over 13.5% of groundwater, 8.52% of surface water, and 4.4% of both water sources in the sub-basin are challenged with high pollution risks, with approximately 17.47% of the population residing in moderately risked areas. Additionally, 5.64%, 3.88%, and 2.30% of the population face high risks specifically related to groundwater pollution (GWPR), surface water pollution (SWPR), and overall water pollution (WSPR), respectively. Moreover, the Water Pollution Index (WPI) values computed for the dry season surpassed 1 for all ten monitoring sites, indicating a state of pollution in the surface water. These findings serve as a request of action for robust policy measures, improved regulatory frameworks, and community awareness initiatives to address the identified sources of pollution and safeguard the quality of both surface water and groundwater for the well-being of ecosystems and human populations in the studied regions. This involves the incorporation of public

health considerations into Integrated Water Supply Management (IWSM), revising regulations, strategically allocating resources, prioritizing interventions, delineating water protection zones, and providing inputs for environmental impact assessments related to new investments. The identified roles and responsibilities of different sectors further contribute to a holistic understanding of the water quality landscape. Additionally, the integration of these findings with other approaches and models, coupled with the prediction of health risks associated with water quality in the sub-basin, highlights the dominant importance of considering public and ecosystem health issues in IWSM including source control, treatment technologies, and regulatory measures for sustainable and resilient water management practices.

References

1. Bunch, M. J., Parkes, M., Zubrycki, K., Venema, H., Hallstrom, L., et al. (2014). Watershed management and public health: An exploration of the intersection of two fields as reported in the literature from 2000 to 2010. Environmental management, 54, 240-254.
2. Parkes, M. W., Morrison, K. E., Bunch, M. J., Hallström, L. K., Neudoerffer, R. C., et al. (2010). Towards integrated governance for water, health and social–ecological systems: The watershed governance prism. Global Environmental Change, 20(4), 693-704.
3. Mena-Rivera, L., Salgado-Silva, V., Benavides-Benavides, C., Coto-Campos, J. M., & Swinscoe, T. H. (2017). Spatial and seasonal surface water quality assessment in a tropical urban catchment: Burío River, Costa Rica. Water, 9(8), 558.
4. Nguyen, H. Q., Radhakrishnan, M., Huynh, T. T. N., Baino-Salingay, M. L., Ho, L. P., et al. (2017). Water quality dynamics of urban water bodies during flooding in Can Tho City, Vietnam. Water, 9(4), 260.
5. Ye, L., Cai, Q. H., Liu, R. Q., & Cao, M. (2009). The influence of topography and land use on water quality of Xiangxi River in Three Gorges Reservoir region. Environmental Geology, 58, 937-942.
6. Postigo, C., Martinez, D. E., Grondona, S., & Miglioranza, K. S. B. (2018). Groundwater pollution: sources, mechanisms, and prevention.
7. Eba, A. E. L., Kouamé, K. J., Jourda, J. P., Aké, G. E., Saley, M. B., et al. (2013). Demarcation of surface water protection perimeters by using GIS: case of gagnoa reservoir in west central of Côte d'Ivoire. International Journal of Scientific & Engineering Research, 4(4), 1311-1320.
8. Aller, L., Bennett, T., Lehr, J. H., & Petty, R. J. (1985). DRASTIC: a standardized system for evaluating groundwater pollution using hydrogeologic settings.-US EPA/Robert S. Kerr Environmental Research Laboratory. EPA/600/2-85/018, 163 p.
9. Muhammad, A. M., Zhonghua, T., Dawood, A. S., & Earl, B. (2015). Evaluation of local groundwater vulnerability based on DRASTIC index method in Lahore, Pakistan. Geofísica internacional, 54(1), 67-81.
10. WHO. WHO | Global status report on water safety plans. Who [Internet]. 2017;44 pp.
11. Degefu, F., Lakew, A., Tigabu, Y., & Teshome, K. (2013). The water quality degradation of upper Awash River, Ethiopia. Ethiopian Journal of Environmental Studies and Management, 6(1), 58-66.
12. Awoke, A., Beyene, A., Kloos, H., Goethals, P. L., & Triest, L. (2016). River water pollution status and water policy scenario in Ethiopia: raising awareness for better implementation in developing countries. Environmental management, 58, 694-706.
13. Itanna, F. (2002). Metals in leafy vegetables grown in Addis Ababa and toxicological implications. Ethiopian Journal of Health Development, 16(3), 295-302.
14. Hemel, R., & Loijenga, H. (2013). Set up of a Water Governance Program in the Awash River Basin, Central Ethiopia [Assessment of Water Governance Capacity in the Awash River basin Report], Water Governance Centre (WGC): Den Haag. Report, Water Governance Centre.
15. Awoke, A., Beyene, A., Kloos, H., Goethals, P. L., & Triest, L. (2016). River water pollution status and water policy scenario in Ethiopia: raising awareness for better implementation in developing countries. Environmental management, 58, 694-706.
16. Gong, J., Guo, X., Yan, X., & Hu, C. (2023). Review of urban drinking water contamination source identification methods. Energies, 16(2), 705.
17. Nanesa, K. (2021). Awash River's the ongoing irrigation practices, future projects and its impacts on the environment of Awash River Basin. Irrig. Drain. Syst. Eng, 10.
18. Krauer, J., Fries, M., Gämperli, U., Hodel, E., Kassawmar, T., et al. (2014). EthioGIS-2 data catalog: National geospatial database system Ethiopia.
19. Water and Land Resources Information System (WALRIS). WLRC/CDE: National Geospatial database System EthioGIS-3/Release 2019 [Internet]. [Cited 2024 Jan 12].
20. LP DAAC - MOD16A3GF [Internet]. [Cited 2022 Feb 13].
21. Elçi ALPER. NU SC. J Contam Hydrol [Internet]. 2017.
22. Krishna R, Science E, Group E, Iqbal J, Science E, Group E, et al. HHS Public Access. 2015;5(4):345–58.
23. Bishop, M. P., Björnsson, H., Haeberli, W., Oerlemans, J., Shroder, J. F., et al. (2011). Encyclopedia of snow, ice and glaciers. Springer Science & Business Media.
24. Scbwartz F, Sons JWG. Physical and Chemical.
25. Al-Adamat, R. (2017). Modelling surface water susceptibility to pollution using GIS. Journal of Geographic Information System, 9(3), 293-308.
26. Sivertun, A., Reinelt, L. E., & Castensson, R. (1988). A GIS method to aid in non-point source critical area analysis. International Journal of Geographical Information System, 2(4), 365-378.
27. Sivertun, Å., & Prange, L. (2003). Non-point source critical area analysis in the Gisselö watershed using GIS. Environmental Modelling & Software, 18(10), 887-898.
28. Wick, K., Heumesser, C., & Schmid, E. (2012). Groundwater nitrate contamination: factors and indicators. Journal of environmental management, 111, 178-186.
29. Wang, J., He, J., & Chen, H. (2012). Assessment of groundwater contamination risk using hazard quantification, a modified DRASTIC model and groundwater value, Beijing Plain, China. Science of the total environment, 432, 216-226.
30. Mahvi, A. H., Nouri, J., Babaei, A. A., & Nabizadeh, R. (2005). Agricultural activities impact on groundwater

nitrate pollution. International Journal of Environmental Science & Technology, 2, 41-47.
31. Jiao, X., Maimaitiyiming, A., Salahou, M. K., Liu, K., & Guo, W. (2017). Impact of groundwater level on nitrate nitrogen accumulation in the vadose zone beneath a cotton field. Water, 9(3), 171.
32. Pawar, N. A., & Shaikh, I. J. (1995). Nitrate pollution of ground waters from shallow basaltic aquifers, Deccan Trap Hydrologic Province, India. Environmental Geology, 25, 197-204.
33. Torfs P. A Global Assessment of Nitrate Contamination in Groundwater. 2015; (January):1–27.
34. Adnew Degefu, M., Assen, M., Satyal, P., & Budds, J. (2020). Villagization and access to water resources in the Middle Awash Valley of Ethiopia: implications for climate change adaptation. Climate and Development, 12(10), 899-910.
35. Karaouzas, I., Kapetanaki, N., Mentzafou, A., Kanellopoulos, T. D., & Skoulikidis, N. (2021). Heavy metal contamination status in Greek surface waters: A review with application and evaluation of pollution indices. Chemosphere, 263, 128192.
36. Reta, G., Dong, X., Li, Z., Bo, H., Yu, D., et al. (2019). Application of Single Factor and Multi-Factor Pollution Indices Assessment for Human-Impacted River Basins: Water Quality Classification and Pollution Indicators. Nature Environment & Pollution Technology, 18(3).
37. Dawood, A. S. (2017). Using of Nemerow's Pollution Index (NPI) for water quality assessment of some Basrah Marshes, South of Iraq. Journal of Babylon University/ Engineering Sciences, 25(5), 1708-1720.
38. Xu, H., Gao, Q., & Yuan, B. (2022). Analysis and identification of pollution sources of Comprehensive River water quality: Evidence from two river basins in China. Ecological Indicators, 135, 108561.
39. Raharjo, M. (2020). Water Pollution Index (WPI) and Incidence of Diarrhea among Children Under Five Years Old in Coastal Area of Semarang City, Indonesia. In E3S Web of Conferences (Vol. 202, p. 05022). EDP Sciences.
40. Su, K., Wang, Q., Li, L., Cao, R., Xi, Y., et al. (2022). Water quality assessment based on Nemerow pollution index method: A case study of Heilongtan reservoir in central Sichuan province, China. PloS one, 17(8), e0273305.
41. Effendi, H. (2016). River water quality preliminary rapid assessment using pollution index. Procedia Environmental Sciences, 33, 562-567.
42. Haque, M. M., Niloy, N. M., Nayna, O. K., Fatema, K. J., Quraishi, S. B., et al. (2020). Variability of water quality and metal pollution index in the Ganges River, Bangladesh. Environmental Science and Pollution Research, 27, 42582-42599.
43. Su, K., Wang, Q., Li, L., Cao, R., & Xi, Y. (2022). Water quality assessment of Lugu Lake based on Nemerow pollution index method. Scientific Reports, 12(1), 13613.
44. Hossain, M., & Patra, P. K. (2020). Water pollution index–A new integrated approach to rank water quality. Ecological Indicators, 117, 106668.
45. Kong, M., Zhong, H., Wu, Y., Liu, G., Xu, Y., et al. (2019). Developing and validating intrinsic groundwater vulnerability maps in regions with limited data: a case study from Datong City in China using DRASTIC and Nemerow pollution indices. Environmental earth sciences, 78, 1-14.
46. Allouche, N., Maanan, M., Gontara, M., Rollo, N., Jmal, I., et al. (2017). A global risk approach to assessing groundwater vulnerability. Environmental Modelling & Software, 88, 168-182.
47. Zarei, M., Sedehi, F., & Raeisi, E. (2014). Hydrogeochemical characterization of major factors affecting the quality of groundwater in southern Iran, Janah Plain. Geochemistry, 74(4), 671-680.
48. Azagegn, T., Asrat, A., Ayenew, T., & Kebede, S. (2015). Litho-structural control on interbasin groundwater transfer in central Ethiopia. Journal of African Earth Sciences, 101, 383-395.
49. Oke, S. A., & Fourie, F. (2017). Guidelines to groundwater vulnerability mapping for Sub-Saharan Africa. Groundwater for Sustainable Development, 5, 168-177.
50. Fatemi H. GROUNDWATER VULNERABILITY MAPPING OF THE ADDIS ABABA WATER SUPPLY AQUIFERS,
51. Ehirim C, Nwankwo C. Evaluation of aquifer characteristics and groundwater quality. Arch Appl Sci Res [Internet]. 2010; 2(2):396–403.
52. Foster, S., Hirata, R., & Andreo, B. (2013). The aquifer pollution vulnerability concept: aid or impediment in promoting groundwater protection?. Hydrogeology Journal, 21(7), 1389.
53. Yitbarek, A., Razack, M., Ayenew, T., Zemedagegnehu, E., & Azagegn, T. (2012). Hydrogeological and hydrochemical framework of Upper Awash River basin, Ethiopia: with special emphasis on inter-basins groundwater transfer between Blue Nile and Awash Rivers. Journal of African Earth Sciences, 65, 46-60.
54. Voisin, J., Cournoyer, B., Vienney, A., & Mermillod-Blondin, F. (2018). Aquifer recharge with stormwater runoff in urban areas: Influence of vadose zone thickness on nutrient and bacterial transfers from the surface of infiltration basins to groundwater. Science of the Total Environment, 637, 1496-1507.
55. Taddese, G. (2001). Land degradation: a challenge to Ethiopia. Environmental management, 27, 815-824.
56. Hamilton, L. S., Dudley, N., Greminger, G., Hassan, N., Lamb, D., et al. (2008). A thematic study prepared in the framework of the Global Forest Resources Assessment 2005.
57. Ruffeis, D., Loiskandl, W., Spendlingwimmer, R., Schonerklee, M., Awulachew, S. B., et al. (2008). Environmental impact analysis of two large scale irrigation schemes in Ethiopia.
58. Wang, X. (2001). Integrating water-quality management and land-use planning in a watershed context. Journal of environmental management, 61(1), 25-36.
59. Desta, H., Lemma, B., & Gebremariam, E. (2017). Identifying sustainability challenges on land and water uses: The case of Lake Ziway watershed, Ethiopia. Applied Geography, 88, 130-143.
60. Tanaka, M. O., de Souza, A. L. T., Moschini, L. E., & de Oliveira, A. K. (2016). Influence of watershed land use and riparian characteristics on biological indicators of stream water quality in southeastern Brazil. Agriculture,

Ecosystems & Environment, 216, 333-339.
61. Authority AB, Werer M. AWASH BASIN SEDIMENTATION MODELING PROJECT Study Report Working Package – II Land Use Land Cover analysis Study Team Members : 2017;1–94.
62. Tadese, M., Kumar, L., Koech, R., & Kogo, B. K. (2020). Mapping of land-use/land-cover changes and its dynamics in Awash River Basin using remote sensing and GIS. Remote Sensing Applications: Society and Environment, 19, 100352.
63. Somaratne, N., Zulfic, H., Ashman, G., Vial, H., Swaffer, B., et al. (2013). Groundwater risk assessment model (GRAM): groundwater risk assessment model for well-field protection. Water, 5(3), 1419-1439.
64. Kawo, N. S., & Karuppannan, S. (2018). Groundwater quality assessment using water quality index and GIS technique in Modjo River Basin, central Ethiopia. Journal of African Earth Sciences, 147, 300-311.
65. Duda, R., Klebert, I., & Zdechlik, R. (2020). Groundwater pollution risk assessment based on vulnerability to pollution and potential impact of land use forms. Pol. J. Environ. Stud, 29(1), 87-99.
66. Devic, G., Djordjevic, D., & Sakan, S. (2014). Natural and anthropogenic factors affecting the groundwater quality in Serbia. Science of the Total Environment, 468, 933-942.
67. Kayode, O. T., Okagbue, H. I., & Achuka, J. A. (2018). Water quality assessment for groundwater around a municipal waste dumpsite. Data in Brief, 17, 579-587.
68. Karroum, M., Elgettafi, M., Elmandour, A., Wilske, C., Himi, M., et al. (2017). Geochemical processes controlling groundwater quality under semi-arid environment: a case study in central Morocco. Science of the Total Environment, 609, 1140-1151.
69. Yaghi, Y., & Salim, H. (2017). Integration of Rs/gis for surface water pollution risk modeling. Case study: Al-Abrash Syrian coastal basin. The International Archives of the Photogrammetry, Remote Sensing and Spatial Information Sciences, 42, 949-954.
70. Teklu, B. M., Adriaanse, P. I., Ter Horst, M. M., Deneer, J. W., & Van den Brink, P. J. (2015). Surface water risk assessment of pesticides in Ethiopia. Science of the Total Environment, 508, 566-574.
71. Degefu, F., Lakew, A., Tigabu, Y., & Teshome, K. (2013). The water quality degradation of upper Awash River, Ethiopia. Ethiopian Journal of Environmental Studies and Management, 6(1), 58-66.
72. Owa, F. W. (2014). Water pollution: sources, effects, control and management. International Letters of Natural Sciences, 3.
73. Elumalai, V., Brindha, K., & Lakshmanan, E. (2017). Human exposure risk assessment due to heavy metals in groundwater by pollution index and multivariate statistical methods: a case study from South Africa. Water, 9(4), 234.
74. Mersha, A. N., Masih, I., De Fraiture, C., Wenninger, J., & Alamirew, T. (2018). Evaluating the impacts of IWRM policy actions on demand satisfaction and downstream water availability in the upper Awash Basin, Ethiopia. Water, 10(7), 892.
75. Water, S. D. (2004). From Source to Tap: Guidance on the.
76. Engineer WQ, Water a, Engineers I. HAZARD ANALYSIS AND CRITICAL CONTROL POINTS Paper Presented by : Kevin Hellier HAZARD ANALYSIS AND CRITICAL CONTROL POINTS. Water. 2000; (101):101–9.
77. Josephson, A. L., Ricker-Gilbert, J., & Florax, R. J. (2014). How does population density influence agricultural intensification and productivity? Evidence from Ethiopia. Food Policy, 48, 142-152.
78. Abebe, Y., Alamirew, T., Whitehead, P., Charles, K., & Alemayehu, E. (2023). Spatio-temporal variability and potential health risks assessment of heavy metals in the surface water of A wash basin, Ethiopia. Heliyon, 9(5).
79. Assegide, E., Alamirew, T., Dile, Y. T., Bayabil, H., Tessema, B., et al. (2022). A synthesis of surface water quality in A wash Basin, Ethiopia. Frontiers in water, 4, 782124.
80. Naz, A., Chowdhury, A., Mishra, B. K., & Gupta, S. K. (2016). Metal pollution in water environment and the associated human health risk from drinking water: A case study of Sukinda chromite mine, India. Human and Ecological Risk Assessment: An International Journal, 22(7), 1433-1455.
81. Talema, A. (2023). Causes, negative effects, and preventive methods of water pollution in Ethiopia. Quality Assurance and Safety of Crops & Foods, 15(2), 129-139.
82. Babuji, P., Thirumalaisamy, S., Duraisamy, K., & Periyasamy, G. (2023). Human health risks due to exposure to water pollution: a review. Water, 15(14), 2532.
83. Chen, Q., Mei, K., Dahlgren, R. A., Wang, T., Gong, J., et al. (2016). Impacts of land use and population density on seasonal surface water quality using a modified geographically weighted regression. Science of the total environment, 572, 450-466.
84. Wang, G., Mang, S., Cai, H., Liu, S., Zhang, Z., et al. (2016). Integrated watershed management: evolution, development and emerging trends. Journal of Forestry Research, 27, 967-994.
85. Tromboni, F., Dilts, T. E., Null, S. E., Lohani, S., Ngor, P. B., et al. (2021). Changing land use and population density are degrading water quality in the Lower Mekong Basin. Water, 13(14), 1948.